

Dictyostelium Chemotactic Response to Spatial and Temporal Gradients. Theories of the Limits of Chemotactic Sensitivity and of Pseudochemotaxis

R.P.Futrelle

Biology and Computing Research Group, Department of Genetics and Development, University of Illinois, Urbana, Illinois 61801

Four aspects of ameboid cell chemotaxis are discussed: 1) Ameboid cells (*Dictyostelium discoideum*, leukocytes) might orient to chemotaxin gradients by sensing a spatial gradient or a temporal change in the concentration. Using a moving micropipette source of cAMP, we show the *D* discoideum cells can orient toward a gradient in which the concentration is everywhere decreasing with time—implying a spatial mechanism. 2) The number of molecules N that must be released by a source to orient a cell is limited by the natural concentration “noise” due to diffusion. N is shown to be simply related to the cell size and the distance from the source. 3) We show that previous diffusion equations for cell population movement have not taken the speed variations (klinokinesis) into account properly, and we present a new result that does. 4) We briefly discuss reaction-diffusion models of cell orientation.

Key words: cell diffusion, cell motion, cellular slime mold, chemotaxis, *Dictyostelium discoideum*, klinokinesis, orientation response, pseudochemotaxis, reaction-diffusion models, receptor noise

As a bacterial cell moves through a chemotaxin gradient in solution, it monitors the time rate of change of the concentration it sees. It reacts differently to rising and falling concentrations, and by biasing its otherwise random motion appropriately, it moves toward an attractant source—it shows chemotaxis. This is a temporal mechanism [1]. The method used by an ameboid cell to achieve chemotaxis is not understood. It could be temporal or it could operate by direct measurement of the spatial gradient over the cell [2, 3]. To probe the mechanism, we presented a

Received August 4, 1981, accepted September 30, 1981.

stimulus in which a spatial gradient is present but the concentration seen by the cells was decreasing with time. The spatial mechanism would direct the cells up the gradient. The temporal mechanism would not support motion of the cells up the gradient because each would find a smaller and smaller concentration, the longer it continued up the gradient. We produced the stimulus by exposing *Dictyostelium discoideum* cells to a moving micropipette source of the chemoattractant cAMP in a liquid-filled chamber. Computer analysis of the motion of a number of cells showed that they moved up the spatial gradient, giving strong support to a spatial, rather than a temporal mechanism. In natural aggregation, the cells are presented with a decreasing but attractant gradient as the cAMP wave propagates past them. Cells do not reverse in such a situation. To reconcile our observations with those of aggregation we must assume that the strength and shape of the natural wave must be such that the reversal is suppressed. Recent measurements of cAMP relaying in "concentration clamp" experiments suggest that the exact dose and timing does affect adaptation to the stimulus [4, 5].

Another aspect of the temporal vs spatial sensing models is revealed by studying the molecular signal presented to a cell. Building on the work of Berg and Purcell [3], we show that the information available to a cell is limited by fluctuations in the microscopic concentration of the chemotaxin molecules [6]. This limits the ability of the cell to orient properly when the concentration or gradient is weak. This limitation is independent of the particular cellular sensing mechanism (spatial or temporal). We then suggest how the information provided by receptor occupancy might be used to organize the motility machinery of the cell to give oriented movement [7].

Finally, we discuss the movement or "diffusion" of whole cell populations. In certain assays, questions arise as to whether cell movement and accumulation is due to true oriented motion, ie, chemotaxis, or merely to the fact that the cell speed varies as a function of the concentration of the agent being tested [8, 9, 10, 11]. A simple but carefully drawn model of the second effect, pseudochemotaxis, [11], shows that past models have overlooked important qualitative aspects of the motion. This exercise shows how sensitive the entire analysis is to seemingly innocent assumptions in the models. It casts some doubts on our ability to draw conclusions from the overall motion of populations. Detailed analysis of single cell motions under controlled conditions should be more informative.

METHODS

Cell Preparations

Dictyostelium discoideum/B were grown with *Escherichia coli* and harvested at maximum yield, 42 h. After washing and resuspending in Bonner's Salt Solution (BSS), the cells were allowed to settle in an inverted coverslip chamber (Fig. 1) at 1,100/mm². The cells were stimulated in the chamber after 24 h. Some aggregation was occurring in the chamber at this time.

Stimulation

A glass micropipette (Haer Omega-Dot, 1.2 mm OD) was pulled to a tip inner diameter of about 0.6 μm and then bent in a microforge (Fig. 2). The pipette was filled with 10⁻⁵M cAMP, diffusion constant $D=10^{-5}\text{cm}^2/\text{s}$. This resulted in a release rate estimated at 6×10^3 molecules/s or 10⁻²⁰ moles/s (this is a rough estimate,

see Discussion for details.) The pipette was held in a micromanipulator (Leitz). The pipette was then swept past the cells eight times. For each sweep cycle, the pipette was positioned at the right edge of the field (as viewed), 30 μm below the coverslip; it was then moved 15 μm to the left (minus x -direction) after each film frame exposure (eyepiece reticle used for alignment), giving a speed of 120 $\mu\text{m}/\text{min}$; after about 350 μm of movement, the pipette was quickly dropped to about 150 μm below the coverslip and moved within a few seconds back to the starting point. This sequence resulted in a sweep every 3 min. The pipette produced a moving "wave" of concentration as it passed over the cells. The concentration, $c(x)$, seen by the cells

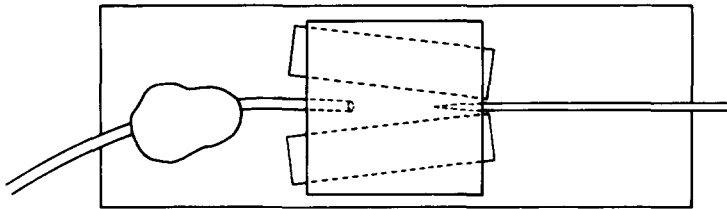


Fig. 1. Cell chamber (top view). The chamber was built on a 1" \times 3" glass slide. Two pieces of glass were cut from the end of a slide and fastened to the base slide with silicone cement to form a tapered chamber. A 22-mm square coverslip was laid on top and held on with a small amount of Vaseline. The chamber volume is about 100 μl . Water evaporated from the chamber at 30 $\mu\text{l}/\text{h}$ and was replaced with distilled water from a siphon tube (at left) held in position with Plasticene and running to a flask. The taper of the chamber together with capillary action assures that water addition or loss produces a change in the meniscus position on the left but has little effect on the meniscus in the small (1 mm) opening on the right. The cell suspension was inserted into the chamber when it was inverted so that the cells attached to the coverslip. The chamber was held by a conventional slide stage and the micropipette (Fig. 2) entered and left the chamber through the meniscus in the small right hand opening.

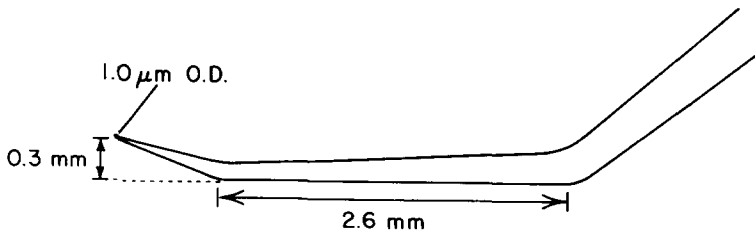


Fig. 2. Stimulation micropipette (side view). A glass fiber capillary was pulled with a long taper to a tip OD of 1.2 μm and then bent twice on a microforge. The bend near the tip was made by differential heating. The bend in the larger section was made by applying mechanical pressure to the pipette with a jeweler's screwdriver, pushing the pipette close to the heated filament. The design is a compromise that allows reasonable optical quality, adequate horizontal and vertical working distance, and ease of backfilling.

can be calculated to an excellent approximation by assuming that the pipette started very far (infinitely far) from the cells. With this assumption the concentration seen at a cell can be obtained in closed form:

$$c(x) = \frac{R}{2\pi D r} \exp [(x-r)v/2D], \quad (1)$$

where R is the rate of release from the pipette (molecules/s), D is the diffusion constant, r is the distance from pipette tip to the cell in question, x is the x -distance of the cell from the pipette x position, and v is the speed at which the pipette moves. This shows that the concentration seen by the cell at any moment is a function only of the distances x and r at that moment and does not involve the time explicitly. (In deriving equation 1, it was assumed that the cells are on an impermeable substrate. The concentration seen by the cell is therefore double that of the solution of the diffusion equation in unbounded three-dimensional space. In our chamber, the substrate is glass. On agar the situation is similar; diffusion occurs within the agar and the liquid film on top and the "impermeable substrate" that blocks diffusion is the air above the agar.)

Data Analysis

Sixteen-millimeter color films were made at 8 frames/min with Zernike phase contrast optics, $40\times$ magnification to the film. Forty-three cells whose initial positions were within $50\ \mu\text{m}$ of the path of the pipette (projected on the glass) were tracked and their x,y positions entered using the Galatea/ST system. The velocity value of each cell in each frame was labeled by its x distance from the pipette in that frame. These data were sorted into ten groups according to these x values. For example, all cells with x between $53\ \mu\text{m}$ and $106\ \mu\text{m}$ had their v velocities averaged together and the resultant value (divided by the overall mean speed of $7.9\ \mu\text{m}/\text{min}$) was plotted at $x=80\ \mu\text{m}$.

Extensive details about the methods can be found in a paper by Futrelle et al [12].

RESULTS

The results are shown in Figure 3. The cells to the left of the pipette, to the left of the center on the plot, moved to the right (the x component of their velocity is positive) and reached about half the mean speed. These cells moved toward an attractant gradient and toward a concentration which increased with time. As the wave moved past the cells, they were exposed to a reversed gradient in which the concentration was falling with time. These cells, to the right of the center on the plot, showed a weak but unambiguous reversal; the x component of their velocity became negative. In viewing the film, it was clear that some cells reversed noticeably, others did not reverse at all. (An obvious alternative would have been for all the cells to have reversed weakly.)

DISCUSSION

The stimulus is discussed first: If a pipette is placed in front of a group of cells and then suddenly moved and placed behind them, a reversed gradient is created. However, the second or reversed gradient produces a concentration at the cells

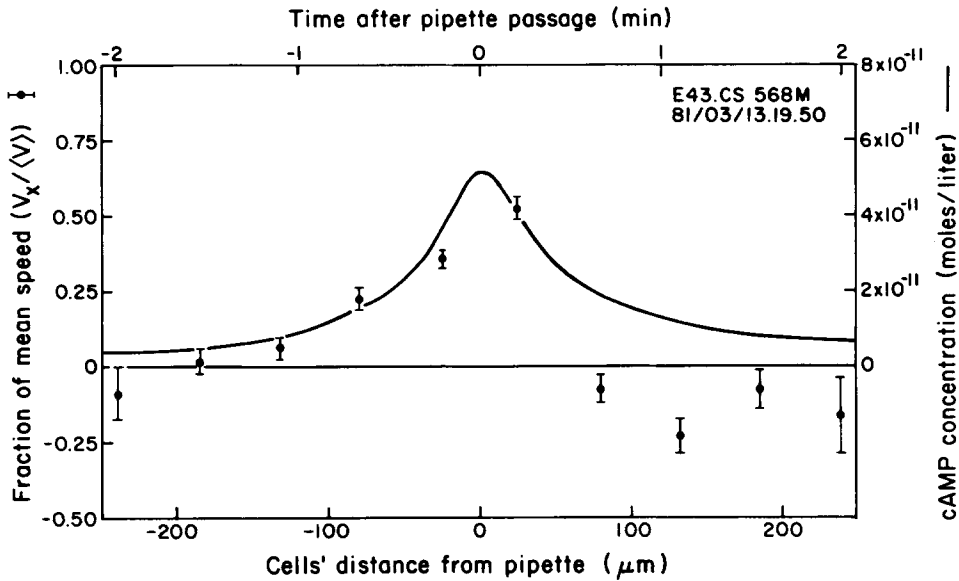


Fig. 3. cAMP stimulus wave (right ordinate) and cell velocity response (left ordinate). The data was averaged over eight sweeps in which the pipette was moved from right to left at $120 \mu\text{m}/\text{min}$. Each velocity point (x -velocity component as a fraction of the grand mean cell speed) averages in it all cells which were a certain x -distance from the pipette (see Methods). Since the pipette was moved at a constant speed, a cell at a certain x -distance from the pipette had a fixed time at which the pipette passed through the cell's location. These time values are plotted on the upper scale. The error bars shown are ± 2 SEM. The number of data included in the average varied from 44 for the right-hand point to 568 for the point at $-26 \mu\text{m}$.

that increases with time. This sort of stimulation creates two brief "waves" in succession, coming from opposite directions. This is analogous to two natural centers competing alternately for the group of cells. In the moving wave we created a reversed gradient which had a concentration that *decreased* with time.

Equation 1 for this moving concentration wave can be understood intuitively. If the speed v is set to zero, the static case, the exponential becomes 1 and the standard concentration field from a fixed steady point source is obtained. For any nonzero speed, the exponent can be written in the simple form $(x-r)/L$, where L is the characteristic distance $2D/v$. In our experiment, $L=500 \mu\text{m}$. For all cell distances from the pipette appreciably less than L , the exponential is close to 1, and the static result is recovered. That is, the standard static concentration field is moved along as a "rigid" entity tied to the pipette location. For distances of the order of L or greater, the solution deviates noticeably from the standard one. Note, for example, that the concentration at the right edge of Figure 3, where the pipette has already passed, is higher than that at the left edge, where the pipette has yet to pass, as one might expect. Since the total distance from cell to pipette, r , is always greater than one of its components, x , the exponent in Equation 1 will always be negative. Thus, the concentration at a cell is always less than what would

be obtained if the pipette were moved very slowly or left in one place indefinitely. Finally, the equation shows that by making the distance between the pipette and the coverslip large (small), it is possible to create a wide (narrow) wave at the cells. The wave will be approximately symmetric as long as it is narrower than L . In this experiment, the speed of the wave ($120 \mu\text{m}/\text{min}$) was appreciably greater than the cell speed ($\approx 8 \mu\text{m}/\text{min}$) so that the cells could never "catch up" with the wave. Wave speeds in natural aggregation vary from $40 \mu\text{m}/\text{min}$ at high cell density to $300 \mu\text{m}/\text{min}$ at low density.

In the liquid-filled chambers used, aggregation was not efficient. There were a few groups of aggregating cells in the chamber at the time the stimulation was done. This tells us that the cells were competent to respond to the natural aggregation signals. The type of pipette used reliably produced a steady molecular flux from the tip. The equation for the concentration $c(r)$ is accurate (ignoring amplification or degradation of cAMP). The pipettes we use put out such a small cAMP flux that absolute calibration is difficult and has not been accomplished entirely satisfactorily as yet. Thus, though the shape of the concentration wave in Figure 3 is accurate, the absolute concentrations are an estimate. That such low concentrations ($< 10^{-10}$ M) could be effective is not unreasonable since leukocytes (similar sized ameboid cells) are known to respond to oligopeptide chemoattractant concentrations of $< 10^{-10}$ M [2]. The result in Figure 3 also shows that the cells reverse in less than a minute, so that they do not have an extensive period of motion refractoriness under this stimulus.

The Signal Required to Orient a Cell

The information that a cell has about the concentration and gradient of a chemotaxin is derived from the cell's receptors, or more specifically, from the moment-to-moment distribution of occupied receptors. Because the experiment above suggests strongly that the spatial gradient is involved in cell orientation, we will focus our attention on modelling the cell's response to such a gradient. We will assume that the gradient is produced by a point source that emits N chemoattractant molecules over a time T . These diffuse out in three dimensions to a spherical cell of radius a , whose center is a distance r from the source (Fig. 4). A fraction of the N molecules diffuse to the surface of the cell. Of the molecules that reach the surface of the cell, only a fraction, e_b , will bind to the receptors, e_b is called the binding efficiency of the cell. These molecules will then be released. They may return and rebind to receptors one or more times, but eventually they all escape from the cell permanently, never to return. On the average, more molecules strike the front of the cell (towards the source) than strike the back. But, in a certain fraction of the experiments, due to the random thermal motion of the chemoattractant molecules, more molecules might hit the back than the front. In this case, unavoidable fluctuations in the environment have caused the "wrong" information to be presented to the cell. Even if the cell acted with perfect reliability in responding to the distribution of occupied receptors, in a certain fraction of the experiments, it would orient away from a chemoattractant source rather than towards it because of the fluctuations. Measurements of various chemosensory phenomena including *E. coli* chemotaxis show that cells operate at or near the absolute limits set

by these fluctuations in the environment. It is therefore necessary to study the sensitivity of spatial gradient sensing in the cellular slime molds and leukocytes to see how closely they approach the absolute limits.

At the low concentrations we are concerned with, each chemoattractant molecule from the source moves independently of the others, the only constraint being that the average number of hits is constrained by the geometry of the problem. Specifically, the total number of molecules from the source hitting the spherical cell and binding to receptors on it is,

$$n_t = e_b N(a/r). \tag{2}$$

Equation 2 is simple, but counterintuitive in certain respects. One might suppose that the number of molecules striking the cell would be proportional to the cell's area, not its linear dimension. It is true that the *total* number of molecular collisions is proportional to the area, but diffusive motion paths are complex, so that the larger the object's area, the more these collisions are due to *the same molecules restriking the surface*. If the cell is assumed to be placed in a constant concentration, a result similar to Equation 2 can be derived: the flux of molecules each striking the surface for the first time is proportional to the linear dimension of the object, not to its area. This result is well known in chemical reaction dynamics where it appears in computations of the diffusive on-rate of unreacted molecules to a reactive site. A derivation of Equation 2 can be found in the elegant paper of Berg and Purcell [3], which was the inspiration for a number of the developments reported in this paper.

For our point source example, the difference in the number of molecules hitting the front hemisphere of the cell, n_+ , and the number hitting the back, n_- , can be shown to be, on the average

$$\Delta n = n_+ - n_- = n_t(a/r). \tag{3}$$

Since $n_+ + n_- = n_t$,

$$n_+ = (n_t + \Delta n)/2 \tag{4a}$$

$$n_- = (n_t - \Delta n)/2. \tag{4b}$$

These are average values. We now must calculate the fluctuations around the averages. The molecules first striking the front surface are independent of those first striking the back so that, strictly, the error variances are additive. (In this type of analysis, we do not count restrikes and rebinding to receptors by the same chemotaxin molecules as new sources of information to the cell about its surroundings. This point was made by Berg and Purcell.) The variance of Δn is therefore

$$\sigma_{\Delta n}^2 = \sigma_{n_+}^2 + \sigma_{n_-}^2. \tag{5}$$

Since the individual strikes are independent (Poisson) random variables, the variances obey the square-root-of-n law. (As Schrödinger has pointed out, it is the

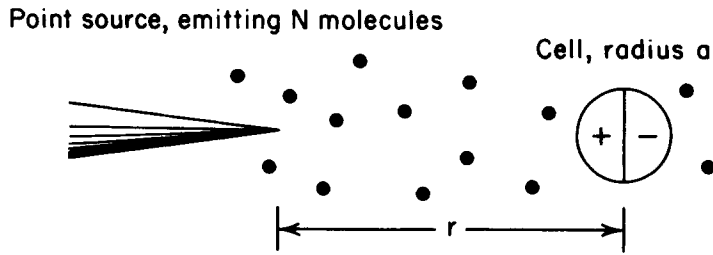


Fig. 4. Geometry of a localized source emitting N molecules over time T , some of which strike the cell of radius a at a distance r away. The cell compares the concentrations on its $+$ and $-$ sides to detect the gradient.

square-root-of- n law that allows large systems to exhibit orderly behavior [13].) To a good approximation (neglecting the slight difference between n_+ and n_- in the typical case),

$$\sigma_{n_+} = \sigma_{n_-} = \sqrt{n_t/2}. \quad (6)$$

The result is that the error in the difference is

$$\sigma_{\Delta n} = n_t^{1/2}. \quad (7)$$

The difference, Δn , that the cell is trying to measure, equation 3, is typically a small fraction of the total strikes n_t , but the error, $\sigma_{\Delta n}$, in this measurement, equation 7, can be substantial, since it is related to the total number of new strikes on the cell. But since the difference is proportional to n_t and the error is proportional to the square root of n_t , it is possible to make n_t large enough to achieve a small relative error in the difference, that is, in the measurement of the gradient. This can be done by making N large, a large, or r small. To estimate this we form the signal-to-noise ratio (SNR), with Δn the signal and $\sigma_{\Delta n}$ the noise, and require that the SNR be > 1 ,

$$\text{SNR} = \Delta n / \sigma_{\Delta n} = \Delta n / n_t^{1/2} = e_b N^{1/2} (a/r)^{3/2} > 1. \quad (8)$$

Rearranging this gives the simple result [6],

$$N > \frac{1}{e_b} \left(\frac{r}{a} \right)^3. \quad (9)$$

The simple result of equation 9 states that the number of molecules, N , required to orient a cell is simply related to the binding efficiency, e_b , and to the geometry of the system—the radius a of the cell and its distance r from the source. The result is striking because it does not involve the time course of the signal or the molecular details of the chemotaxin-receptor interaction. To a large extent, the result is actually independent of these details. The implicit assumptions made in the derivation are discussed in the next few paragraphs.

If the cell response is observed after most of the signal molecules have had sufficient time to reach the cell, then the results will be essentially independent of the diffusion constant D and equation 9 will apply. In typical experiments in our lab, diffusion to a cell $75 \mu\text{m}$ from the pipette takes about 6 s and cell responses are monitored after that, eg, at 20 s. In a similar way, the numerical value of the diffusion constant does not affect the fraction of the molecules from the source that hit the cell, or the distribution from front to back, or the magnitude of the fluctuations – all of which enter into the derivation of equation 9.

The time course of the signal will also have no effect on the fraction of molecules that hit the cell, or the distribution, or the fluctuations, once an adequate amount of time has passed. However, if the signal is too brief and strong, it may lead to a high transient concentration at the cell, saturating the receptors so that some of the signal cannot be processed. In the derivation above, we assumed that the binding is linear in the concentration. This is the case when the concentration is below K_d , the dissociation constant, and is quite appropriate for estimating threshold effects – the lowest concentrations at which a cell might respond. If the signal is very prolonged, T large, the cell may not have sufficient quantitative processing stability to “remember” and integrate the early part of the signal and add it to the later part of the signal. Unless it does this, it cannot average over the noise fluctuations to get a reliable indication of the concentration gradient.

The result of equation 9 is also independent of the particular molecular species involved and its interaction with the receptors. The reason for this is that any reasonable chemotaxin-receptor complex has a high dissociation energy, much greater than thermal energy. The interaction is therefore essentially “noise-free” so that, whatever mechanism the cell uses (eg, ion-gating, transmembrane enzyme activation), a substantial signal can be produced inside the cell by the action of a single bound receptor regardless of the details of the interaction. This point has been well illustrated in experiments showing that the moth *Bombyx mori* can detect single pheromone molecules [14].

The result in equation 9 can be derived from the time-oriented approach, equation 60 of Berg and Purcell [3]. To do this, the concentration field is described by equation 1, with the speed v set to 0, ie, the standard stationary source. We make the approximation that the concentration is low enough that the binding is linear (in their terms, $c \ll c_{1/2}$ so that $cc_{1/2}/(c + c_{1/2}) \approx c$.) Then their equation 60 can be written in the form

$$N = RT > \frac{4}{e_b} \left(\frac{r}{a} \right)^3. \tag{10}$$

N , the total number of molecules, is the release rate R times the time T . (The binding efficiency, e_b , is their term $N_s/(N_s + \pi a)$, where N is the number of receptors each with radius s .) The only difference between equations 9 and 10 is the factor 4. This arises because the SNR threshold was chosen differently in their analysis.

The binding efficiency can be calculated from binding kinetics measurements. The total current of new, information-bearing molecules onto the cell is $R_d = 4\pi Dac$. But not all of this current is actually processed by the cell (bound to receptors). In the steady state, the on-rate of binding to receptors, the rate at which molecules are processed, ie, bound to receptors, is equal to the off-rate, and the latter can be measured. The off-rate is equal to the number of receptors occupied, $N_r c / K_d$, times the dissociation rate k_{off} , with N_r the number of receptors and K_d the

dissociation constant (assuming a linear binding regime.) The processing rate is therefore $R_p = N_r c k_{off} / K_d$. The ratio of these two is the binding efficiency, e_b , the fraction of the current onto the cell which binds to any receptors,

$$e_b = R_p / R_d. \tag{11}$$

For the D discoideum high-affinity sites, $N_r \approx 10^4$ receptors/cell, $K_d = 5 \times 10^{-9}$ M [15-17], and $k_{off} = 0.5 \text{ s}^{-1}$ [18]. The cell radius is taken as $5 \mu\text{m}$. This gives the binding efficiency for D discoideum,

$$e_b = 2.5\%. \tag{12}$$

The results of equation 9, 10 and 12 can be compared with cAMP chemotaxis threshold measurements on D discoideum using the small population assay [19]. The measurements at $r = 1 \text{ mm}$ appear to be the most sensitive by our criteria. Using $a = 5 \mu\text{m}$, we can calculate $N > 3.2 \times 10^8$ molecules by equation 9 and $N > 1.3 \times 10^9$ molecules by equation 10. The measured value was 10^{-14} mole or 6×10^9 molecules. Our own measurements [12,20] using a micropipette source touched to agar were made on a scale compatible with actual aggregation, $r = 75 \mu\text{m}$. Orientation was seen within 20 s with $N \approx 10^6$ molecules. (By this time c had reached 2×10^{-10} M at the cells, and Δc across a cell was 13% of c or 2.7×10^{-11} M, similar to the value 3.6×10^{-11} M measured in the small population assay.) Equations 9 and 10 give, respectively, $N > 1.3 \times 10^5$ and $N > 5.4 \times 10^5$. Our own measurements are somewhat uncertain, requiring further calibration (see Discussion), but both measurements are interesting because they suggest that the cells are operating close to the absolute theoretical limits imposed by fluctuations in the environment.

If the signal is appreciably greater than the threshold, $\text{SNR} > 1$, the cell can orient accurately. The angular orientation achievable for a given N can be estimated by comparing the signal Δn seen at perfect orientation ($\theta = 0$ in Fig. 5) with the signal Δn_θ seen at the angle θ . It is the difference between these, $\Delta s = \Delta n - \Delta n_\theta$, which is the "signal," that must be larger than the noise $\sigma_{\Delta n}$. The average value of Δs can be shown to be $\Delta s = \Delta n(1 - \langle \cos \theta \rangle)$, where $\langle \dots \rangle$ indicates an average

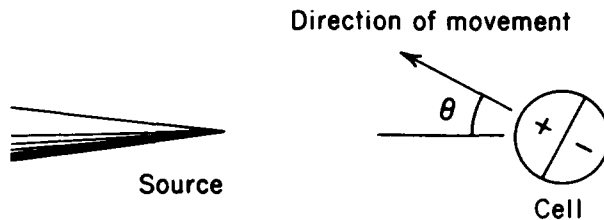


Fig. 5. Cell orientation toward a source. If θ is sufficiently large the cell will detect a significantly smaller difference between its + and - surfaces than it sees when $\theta = 0$. This causes the cell to orient.

over cells or over repetitions of the experiment. Proceeding as before, we find the number of molecules N_θ required to orient to within θ of the direction to the source to be

$$N_\theta > \frac{1}{(1 - \langle \cos\theta \rangle)^2} \frac{1}{e_b} \left(\frac{r}{a} \right)^3. \quad (13)$$

From equation 13, we can find the dependence of the angle on the source strength. This relation takes on its clearest form when the source is strong enough that θ stays close to 0. Then to a good approximation,

$$\langle \theta^2 \rangle \approx 2N_t/N_\theta, \quad (14)$$

where N_t is the threshold value, the rhs of equation 9, and N_θ is the signal orienting the cell. Equation 14 implies, for example, that if the signal N_θ were quadrupled, the root-mean-square angular deviation, $\theta_{\text{rms}} = \langle \theta^2 \rangle^{1/2}$, would drop by a factor of two. Many experiments use fixed, stable gradients to measure chemotactic response, often over a long period of time. In this case, it may be useful to use the theory in the form first derived in [3]. The SNR at a cell presumably does not grow indefinitely with time in such a situation because the cell only averages the signals impinging on it over some limited period of time. (This limited time average would allow it to respond to changing signals.) If the averaging time is so limited, a relation such as equation 13 can still be derived.

In summary, the major results of this section are: 1) The number of molecules required to orient a cell, equation 9, depends only on the cell's binding efficiency and the geometry of the experiment (cell size, source distance) [6]. This generalizes the result of Berg and Purcell which was developed for fixed gradients but estimated the time required to orient. (In fact, most experimental protocols in the past have not been able to set up a stable gradient more rapidly than the cell could orient in the gradient once established, so their form of the theory is difficult to apply.) 2) The cell binding efficiency, e_b , is shown to be an important cellular information processing concept. Its value for *D. discoideum*, $e_b = 2.5\%$, has a major effect on the estimates of actual cell performance. The estimated performance turns out to be very close to the theoretical limit imposed by environmental fluctuations. ($e_b = 50\%$ was assumed in the estimates in [3]). 3) A new and explicit relation between the strength of a source and the accuracy of a cell's angular orientation towards it is derived.

Reaction-Diffusion Models

Meinhardt and Gierer presented an interesting model of cell polarization in a gradient based on their reaction-diffusion equations for pattern formation [21]. The cell was modeled as a ring, a one-dimensional periodic space. An external concentration gradient field stimulated the production of an activator substance and thereby, the production of an inhibitor which diffused rapidly, and in turn, inhibited activator production. This feedback system was such that a weak external gradient could produce a strong cell polarization, which was then resistant to reorientation of the external concentration gradient.

The reaction-diffusion techniques can be extended to the model described in the previous section to develop a more detailed understanding of orientation "noise." Consider the cell modeled as a flat disk moving on a substrate. Each occupied re-

ceptor would cause local synthesis of the activator for as long as it was occupied. To a first approximation we would assume that many molecules of activator were produced per signal molecule bound. This is consistent with the high dissociation energy of the bound complex, which allows it to direct the synthesis of a number of internal signal molecules, or gate the passage of a large number of ions. (If we did not assume this, then the molecular noise problem would be reduplicated inside the cell. But at some point integration must occur, the cell must develop an average response in which the noise of the random association-dissociation reactions on its exterior is smoothed over.) The internal activator and inhibitor gradients could control the inward tension on the membrane as well as the fluidity of the cell membrane. The inward tension would be balanced, on the average, by the cell turgor pressure. The activator and inhibitor levels could also control the establishment and release of cell-substrate attachments (plaques). Higher than average activator levels near one region of the cell boundary could cause the tension to drop and the fluidity to increase. Lower than average levels could increase the tension and also increase the fluidity. The cell would then move in the direction of high activator levels which in turn correspond to high external chemotaxin levels. The (model) cell would thus show a chemotactic response to a weak external chemotaxin gradient. If the cell received an extremely weak orienting signal, the direction of the internal activator gradient direction would fluctuate considerably around the proper direction due to the almost random hits on the receptors. Then the cell would exhibit weak and poorly oriented chemotaxis [7].

A simpler view of this sensory-motor process would be to say that each receptor bound contributes one vectorial piece of information to the cell. That is, each "hit" is assumed to contribute a directional vector drawn from the center of the cell to the hit position. The sum (average) of all the vectors from the n hits is the best estimate the cell has of the orientation of the external gradient. The detailed statistics of this average vector can be worked out.

Albrecht-Buehler has suggested that the various regions of a cell are each capable of carrying out their own autonomous motility activities [22]. If a cell is so organized, then the activator/inhibitor distribution could integrate the regions into a harmonious whole so that the cell would exhibit coordinated, directed motion.

Pseudochemotaxis and the Motion of Cell Populations

A population of cells can often be reasonably approximated as a set of "diffusing particles" of concentration c . It is conventional to assume that the net rate of motion of the cells, the flux J , is proportional to the concentration gradient, which in one dimension is,

$$J = -D \frac{\partial c}{\partial x}, \quad (15)$$

In the general case, D , the cell diffusion "constant," can depend on position. This could typically be due to a gradient of some chemical factor in the substrate, a chemokinetin (or simply kinetin) that would affect the cell speeds, rate of turning, etc. If true chemotaxis is present, there is an additional term proportional to the gradient of the attractant concentration A so that equation 15 becomes

$$J = -D \frac{\partial c}{\partial x} + Bc \frac{\partial A}{\partial x} , \tag{16}$$

where B is an attractant efficiency coefficient [8-11].

When irreversible thermodynamics is used to look rigorously at the forces that drive molecular diffusion currents, more than the concentration gradient can be involved. For example, a temperature gradient, which affects molecular speeds, can drive a molecular or particle current. We will derive an analogous, more general relation for cell populations from a simple model of cell motion with spatially varying speeds and also show how ambiguities may arise in the interpretation of certain experiments.

The situation we wish to model is this: The average speed of any cell is a function of its position only, due to the presence of a kinitin whose concentration c_k in the substrate is not uniform. Others have attempted to model this process but have inadvertently made the cell speed a function of its origin in each random "step." This means that cells in a given region have different average speeds depending on which way they are moving.

We will obtain our results by a transformation of a model whose behavior is simple and well known. This simple one-dimensional lattice model is shown in Figure 6a. Here the diffusing particles are confined to discrete positions Δu apart with n_i particles at lattice point i . At discrete points in time, Δt apart, $\frac{1}{2}n_i$ particles move to point $i + 1$ and $\frac{1}{2}n_i$ move to point $i - 1$. The concentration of particles in the vicinity of u_i is $c_i = n_i/\Delta u$. If we are concerned with time and distance scales sufficiently large compared to Δt and Δu , the appropriate flux equation is equation 15 with $D = \Delta u^2/2\Delta t = D_0$. Using the (rigorous) conservation condition that states that any variation in flux with position must be compensated for by a rise or fall in the concentration, equation 15 gives the conventional diffusion equation,

$$\frac{\partial c(u)}{\partial t} = D_0 \frac{\partial^2 c(u)}{\partial x^2} . \tag{17}$$

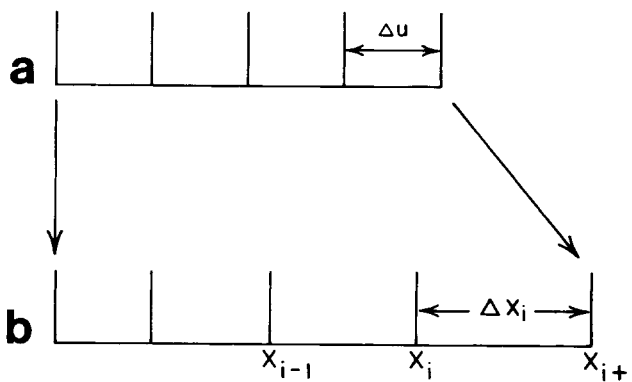


Fig. 6. Correspondence between conventional diffusion on a lattice (a) with the variable step length, and therefore, variable speed model (b). All steps taken in both models are assumed to take the same time Δt . In (b) steps taken between x_i and x_{i+1} in either direction take the same time, so the speed in this region is the same, whatever the origin of the cell.

Now we consider the transformed model shown in Figure 6b. In this model, described in x coordinates, the speed s varies continuously with x . The time for each step is still assumed to be Δt everywhere, so that the spacing, Δx , must vary accordingly. At the discrete points in time, $\frac{1}{2}n_i$ particles move in each direction to populate points $i - 1$ and $i + 1$, just as in the first model. Whatever the details of the speed variation between x_i and x_{i+1} , the times taken to go from x_i to x_{i+1} , or from x_{i+1} to x_i are made rigorously the same, Δt , by the construction of the model. In terms of the number of particles n_i occupying lattice positions in successive steps, the two models are identical. Thus for times $t_j = j \Delta t$,

$$n_i(t_j)_{x\text{-model}} = n_i(t_j)_{u\text{-model}} \tag{18}$$

Since the n solution for the x -model is now known (it is given, in concentration terms, by equation 17), we need only rewrite equation 17 in terms of the appropriate x -coordinates and concentration $c(x)$ to give the diffusion equation for the second, variable speed diffusion model. To do this, it is convenient to define the function $x = f(u)$ which gives the x -position corresponding to a u -position, ie, $x_i = f(u_i)$. The concentrations are related by the derivative of f , which we call $g(x) = df/du$,

$$c(u(x)) = c(x)g(x). \tag{19}$$

The derivatives in equation 17 are related by

$$\frac{\partial}{\partial u} = g(x) \frac{\partial}{\partial x}. \tag{20}$$

We also define the variable diffusion coefficient, $D(x)$, and the variable speed, $s(x)$, by

$$D(x) = g^2(x)D_0, \tag{21}$$

and,

$$s(x) = g(x)\Delta u/\Delta t. \tag{22}$$

With these substitutions, an equation corresponding to equation 17 for $c(u)$ can be obtained and is presented in two equivalent forms,

$$\frac{\partial c(x)}{\partial t} = \frac{\partial}{\partial x} \sqrt{D(x)} \frac{\partial}{\partial x} [\sqrt{D(x)} c(x)]. \tag{23a}$$

$$\frac{\partial c(x)}{\partial t} = \Delta t \frac{\partial}{\partial x} s(x) \frac{\partial}{\partial x} [s(x)c(x)]. \tag{23b}$$

Equation 23 can be compared with the more conventional form which is,

$$\frac{\partial c}{\partial t} = \frac{\partial}{\partial x} D \frac{\partial c}{\partial x}, \tag{24}$$

and the recent form derived by Lapidus,

$$\frac{\partial c}{\partial t} = \frac{\partial^2}{\partial x^2} (Dc). \tag{25}$$

If the cells are allowed to diffuse long enough to come to equilibrium, $\partial c/\partial t \approx 0$, then equations 23,24, and 25 give the respective solutions

$$c(x) \propto 1/s(x) \propto 1/\sqrt{D(x)}, \tag{26a}$$

$$c(x) = \text{const.}, \tag{26b}$$

$$c(x) \propto 1/s^2(x) \propto 1/D(x). \tag{26c}$$

Equation 12 shows that these solutions are qualitatively distinct. But even before equilibrium is reached, equations 23 and 24 have an interesting behavior which can be seen by reexpressing them in the flux formulation. For equation 23 this gives

$$J = -D \frac{\partial c}{\partial x} - \frac{1}{2} c \frac{\partial D}{\partial x} \tag{27a}$$

and for equation 25,

$$J = -D \frac{\partial c}{\partial x} - c \frac{\partial D}{\partial x} \tag{27b}$$

The second terms in both parts of equation 27 have *exactly the same form as a true chemotactic term* such as the one in equation 16. Thus, if cells were spread uniformly ($\frac{\partial c}{\partial x} = 0$) on a substrate that induced a varying cell speed ($\frac{\partial D}{\partial x} \neq 0$), cells would move out of the region of high speed and collect in the region of low speed. In this case, a positive kinetin (speed increasing with concentration) would appear to be repellent and a negative one an attractant. In the extreme case where a high concentration of the kinetin essentially immobilizes the cells, our formulation predicts the classical “trapping effect” ascribed to such situations—the cells will be highly concentrated in the region of low speed. If the cells were started in a localized region, a different type of behavior would ensue. Cells would first appear to diffuse out faster towards the higher D or s region.

General scaling and transformation arguments suggest that our results are of wide applicability. In particular, the result that $c(x) \propto 1/s(x)$ at equilibrium appears to be a general property of any lattice or general stochastic model in which the geometric properties of the particle paths are similar but the speed varies with position.

The moral of the story is that predictions of the behavior of cells under the action of kinetic agents depend crucially on the detailed “microscopic” assumptions made for their behavior, as well as the particular experimental protocol used. The true mechanism of cell behavior (as opposed to our simple models!) is probably best discovered by carefully designed experiments which study the details of individual cell behavior (their paths, speeds, collisions, etc). We must realize that, in evolutionary and functional terms, nature may well blur the distinction between attractant and kinetic effects as long as the cell accumulation or dispersal achieved has the appropriate survival value.

ACKNOWLEDGMENTS

Thanks to J. Anderson, T. Glennon, L. Koryta, S. Sambol, and N. Way for experimental assistance, to S. Zigmond for discussions, R. Lapidus for preprints, and to G. McKee for data analysis. Research supported by NSF PCM79-04242 and the Research Corporation.

REFERENCES

1. Hazelbauer GL, Parkinson JS: In Reissig JL (ed): "Microbial Interactions Receptors and Recognition." London: Chapman and Hall, 1977, series B, vol 3, pp 60-98.
2. Zigmond SH: *J Cell Biol* 77:269, 1978.
3. Berg HC, Purcell EM: *Biophys J* 20:193, 1977.
4. Dinauer MC, Steck TL, Devreotes PN: *J Cell Biol* 86:545, 1980.
5. Dinauer MC, Steck TL, Devreotes PN: *J Cell Biol* 86:554, 1980.
6. Futrelle RP: *Biol Bull* 159:443, 1980.
7. Futrelle RP: Presented at the Workshop on Modeling, 40th Annual Symposium, Soc Dev Biol, Boulder, Colorado, June 6, 1981.
8. Patlak CS: *Bull Math Biophys* 15:311, 1953.
9. Alt W: *J Math Biol* 9:147, 1980.
10. Keller EF: In Jager W, Rost H, Tautu P (eds): "Biological Growth and Spread." (Lecture Notes in Biomathematics). Berlin: Springer-Verlag, 1980, pp 379-387.
11. Lapidus R: *J Theor Biol* 86:91, 1980.
12. Futrelle RP, Traut J, McKee G: *J Cell Biol* (in press).
13. Schrodinger E: "What is Life?" Cambridge: Cambridge University Press, 1967.
14. Kaissling K-E: In Beidler LM (ed): "Handbook of Sensory Physiology. IV. Chemical Senses, Part I." New York: Springer-Verlag, 1971, pp 351-431.
15. Green AA, Newell PC: *Cell* 6:129, 1975.
16. Henderson EJ: *J Biol Chem* 250: 4730, 1975.
17. Klein C, Juliani MH: *Cell* 10:329, 1977.
18. Mullen IA, Newell PC: *Differentiation* 10:171, 1978.
19. Mato JM, Losada A, Nanjundiah V, Konijn TM: *Proc Nat Acad Sci USA* 72:4991, 1975.
20. Futrelle RP, McKee WG, Traut J: *J Cell Biol* 87:57a, 1980.
21. Meinhardt H, Gierer A: *J Cell Sci* 15:321, 1974.
22. Albrecht-Buehler G: *Proc Natl Acad Sci USA* 77:6639, 1980.